



## Original article

# CB2 agonism controls pain and subchondral bone degeneration induced by mono-iodoacetate: Implications GPCR functional bias and tolerance development

Jakub Mlost<sup>a</sup>, Magdalena Kostrzewa<sup>a</sup>, Małgorzata Borczyk<sup>b</sup>, Marta Bryk<sup>a</sup>, Jakub Chwastek<sup>a</sup>, Michał Korostynski<sup>b</sup>, Katarzyna Starowicz<sup>a,\*</sup>

<sup>a</sup> Department of Neurochemistry, Maj Institute of Pharmacology, Polish Academy of Sciences, Smętna 12, 31-343, Cracow, Poland

<sup>b</sup> Department of Molecular Neuropharmacology, Maj Institute of Pharmacology, Polish Academy of Sciences, Smętna 12, 31-343, Cracow, Poland



## ARTICLE INFO

## Keywords:

Osteoarthritis  
CB2  
Functional bias  
MIA  
Analgesia  
Tolerance

## ABSTRACT

**Background and purpose:** The endocannabinoid system became a promising target for osteoarthritis (OA) treatment. Functional selectivity of cannabinoids may increase their beneficial properties while reducing side effects. The aim of the present study was to evaluate the analgesic potential of two functionally biased CB2 agonists in different treatment regimens to propose the best pharmacological approach for OA management.

**Experimental approach:** Two functionally selective CB2 agonists were administered i.p. – JWH133 (cAMP biased) and GW833972A (β-arrestin biased), in a chemically induced model of OA in rats. The drugs were tested in acute and chronic treatment regimens. Analgesic effects were assessed by pressure application measurement and kinetic weight bearing. X-ray microtomography was used for the morphometric analysis of the femur's subchondral bone tissue. Underlying biochemical changes were analysed via RT-qPCR.

**Key results:** Dose-response studies established the effective dose for both JWH133 and GW833972A. In chronic treatment paradigms, JWH133 was able to elicit analgesia throughout the course of the experiment, whereas GW833972A lost its efficacy after 2 days of treatment. Later studies revealed improvement in subchondral bone architecture and decrement of matrix metalloproteinases and proinflammatory factors expression following JWH133 chronic treatment.

**Conclusion and implications:** Data presents analgesic and disease-modifying potential of CB2 agonists in OA treatment. Moreover, the study revealed more pronounced tolerance development for analgesic effects of the β-arrestin biased CB2 agonist GW833972A. These results provide a better understanding of the molecular underpinnings of the anti-nociceptive potential of CB2 agonists and may improve drug development processes for any cannabinoid-based chronic pain therapy.

## 1. Introduction

**Osteoarthritis (OA)** is a chronic joint disease in which cartilage degenerates as a result of its mechanical and biochemical disturbances followed by a low grade inflammatory response [1]. OA is one of the most common disorders causing chronic pain and disability among adults, and it has been recognized by the World Health Organization (WHO) as a “priority disease” (report WHO/EDM/PAR/2004.7) and one of the top 5 healthcare costs in Europe [2]. Although OA is a disease of the whole articulating joint, the proteolytic destruction of cartilage, especially of type II collagen, is a central and irreversible process that

underpins OA. Matrix metalloproteinases (MMPs) are capable of degrading all kinds of extracellular matrix proteins, including collagens, fibronectin and glycoproteins. A series of MMPs, including MMP-13, MMP-2 and MMP-3, play key roles in cartilage destruction in OA through the degradation of aggrecan and collagens [3]. Indeed, multiple MMPs are upregulated in cartilage, serum and synovial fluid of OA patients [4,5], and several pro-inflammatory cytokines such as IL6 and CCL2 induce the expression of MMPs in cartilage [5,6]. In addition to cartilage deterioration, OA is marked by subchondral bone changes, accounted for by osteophyte formation, altered architecture and density as well as changes in mechanical properties [7]. Since bone tissue is

\* Corresponding author.

E-mail address: [starow@if-pan.krakow.pl](mailto:starow@if-pan.krakow.pl) (K. Starowicz).

<https://doi.org/10.1016/j.bioph.2021.111283>

Received 16 November 2020; Received in revised form 11 January 2021; Accepted 12 January 2021

Available online 19 January 2021

0753-3322/© 2021 The Authors.

Published by Elsevier Masson SAS. This is an open access article under the CC BY-NC-ND license

(<http://creativecommons.org/licenses/by-nc-nd/4.0/>).

densely innervated by peripheral sensory neurons, it represents a plausible site for OA pain initiation [8]. Numerous cytokines including IL6 and IL-1 $\beta$  are considered powerful stimulators for osteoclast differentiation and bone resorption [9–11]. Indeed, an imbalance in the subchondral bone remodelling process coupled with increased osteoclasts activity have been correlated with OA progression and pain induction [12].

Unfortunately, the current understanding of OA pathophysiological mechanisms has not led to the development of disease-modifying drugs that are able to stop or slow down disease progression. Present-day treatment is mostly based on palliative care using nonsteroidal anti-inflammatory drugs (NSAIDs) such as ibuprofen, naproxen or diclofenac. Moreover, NSAIDs do not always provide adequate pain relief, and their use is limited because of serious side effects including bleeding, ulcers, stroke, and myocardial infarction [13]. Compelling evidence suggests an active participation of the endocannabinoid system in the pathophysiology of joint pain associated with OA. The endocannabinoid system consists of cannabinoid receptor type 1 (CB1) and cannabinoid receptor type 2 (CB2). CB1 is the most abundantly expressed G-protein coupled receptor (GPCR) in the brain, including the structures involved in pain, reward and cognitive processing. CB2 is widely distributed on immune cells where it is primarily responsible for mediating cytokine release [14]. CB1 agonists were demonstrated to be effective analgesics in various animal models of chronic pain, including OA [15–17]. However, their clinical potential is highly limited by central nervous system-related side effects such as dizziness, memory impairment, euphoria and risk of abuse or addiction [18]. Alternative treatment strategies aimed at CB2 stimulation is devoid of psychoactive potential while retaining the analgesic potential and anti-inflammatory action [19,20]. Moreover, preclinical research has revealed a significant role of CB2 receptors in mediating susceptibility to OA as deletion of the CB2 receptor led to more severe cartilage degeneration in a surgical model of OA [21], possibly due to a reduction of proteoglycan production by chondrocytes. Moreover, chronic treatment with CB2-selective agonist HU308 reduces the severity of OA in the whole joint following surgical induction of OA [21]. It has also been shown that mixed CB1 and CB2 agonist, WIN55,212-2, is able to decrease expression of *Mmp3* and *Mmp13* in chondrocytes *in vitro* [22].

Originally, agonists for GPCRs have been characterized as substances that promote or stabilize conformational changes in the receptor that result in activation of heterotrimeric G proteins and stimulation of second messenger systems. Work over the past two decades, however, has found that agonists can induce distinct “active” receptor conformations that activate only specific subsets of a given receptor’s functional repertoire. In particular, ligands have been identified that exhibit “bias” or “functional selectivity” towards specific G proteins or even other signal transducers such as  $\beta$ -arrestins, a known contributor to GPCR desensitization and internalization [23]. Understanding the impact of these factors on *in vivo* effects may lead to the development of improved biased ligands with the potential to enhance therapeutic benefit while minimizing adverse effects. Encouraging findings concerning the therapeutic potential of CB2 agonists in OA, along with the feasible influence of functional selectivity, prompted us to examine the prolonged anti-nociceptive and disease-modifying potential of CB2 agonists. We designed experiments to compare the behavioural outcome based upon two variables – treatment timing and GPCR functional bias in MIA model, which is well acclaimed model to study analgesic effects of new drugs for osteoarthritis, due cost-effectiveness and preferable time-frame of cartilage degeneration [24]. Moreover, we elucidated the impact of CB2 agonists on subchondral bone morphology and underlying biochemical changes in cartilage. The results presented herein provide a better understanding of the therapeutic potential of CB2 agonists in osteoarthritis by elucidating their molecular mechanism of action.

## 2. Materials and methods

### 2.1. Animals

Male Wistar rats (Charles River, Hamburg, Germany) around the 55th postnatal day, initially weighing 225–250 g, were used for all experiments. The animals were housed as five rats per cage under a standard 12-h/12-h light/dark cycle with food and water available ad libitum. Animals were housed in conventional cages on aspen wood bedding without environmental enrichment. All experiments were approved by the Local Bioethics Committee of the Institute of Pharmacology (Cracow, Poland, approval number 1130/2014 and 125/2018). All pharmacological experiments (including treatment and behavioural assays) were performed in the morning hours (08:00 – 12:00). Animals were sacrificed through decapitation 1 h after drug administration.

### 2.2. Drugs and reagents

JWH133 and GW833972A were obtained from Tocris Bioscience (Bristol, UK) and Carbosynth Ltd (Newbury, UK), respectively. NS398 was obtained from Cayman Europe (Tallinn, Estonia). Mono-iodoacetate (MIA), dimethyl sulfoxide (DMSO) and Kolliphor® EL were obtained from Sigma-Aldrich (Poznan, Poland). JWH133, GW833972A and NS398 were dissolved in a vehicle solution containing 5% DMSO, 5% Kolliphor® EL and 5% ethanol in 0.9 % saline. Organic solvents (DMSO and ethanol) were used to dissolve cannabinoids, and Kolliphor® EL stabilized the emulsion in aqueous solution. Total administration volume for i.p. administration was 2 mL/kg. MIA was dissolved in 0.9 % saline. Dose-response studies were performed to establish the minimum effective dose of GW833972A.

### 2.3. OA induction

Animals were deeply anaesthetized with 5% isoflurane in 100 % O<sub>2</sub> (3.5 L/min) until the flexor withdrawal reflex was abolished. The skin overlying the rear right knee joint was shaved and swabbed with 100 % ethanol. A 27-gauge needle was introduced into the joint cavity through the patellar ligament, and 1 mg of MIA, which is an irreversible NADPH inhibitor, diluted in 50  $\mu$ L of 0.9 % saline was injected into the joint (intra-articular, i.a.) to induce OA-like lesions. MIA inhibits chondrocyte glycolysis and produces cartilage degeneration and subchondral bone alterations producing knee joint lesions and functional impairment similar to that observed in human disease [25]. Sham-treated animals received i.a. administration of 50  $\mu$ L of 0.9 % saline into the right rear knee joint. The age and weight of the animals was selected to allow comfortable access for i.a. injection, whereas only male rats were selected for the experiment to minimize variability related to the estrous cycle throughout the course of the chronic treatment paradigm. The rats were sacrificed at day 28 after MIA injection, as a humane end-point in which the cartilage is no longer able to further degenerate and there is sufficient time to study the effects of prolonged pharmacological treatment. MIA model of osteoarthritis have been chosen due to progressive degeneration of cartilage and subchondral bone, allowing us to study disease-modifying properties of tested drugs. 1 mg of MIA was selected based on our previous findings, which revealed full cartilage degeneration in the given dose [26] and development of pain phenotype that was indistinguishable from the higher dose of 3 mg MIA (data subjected for publication in another paper).

### 2.4. Treatment paradigm

JWH133 (cAMP biased agonist) and GW833972A ( $\beta$ -arrestin biased agonist) were administered i.p. 1 h before the behavioural assessment in three treatment regimens: one acute and two chronic schemes. Time points for acute drug testing were selected based on previous studies [27] that have shown severe development of a pain phenotype and

cartilage destruction from day 21 following OA induction. Thus, acute treatment was performed at day 21 and 28 to establish dose-response effects and the minimum effective dose for subsequent experiments. Two chronic treatment paradigms were used: i) treatment #1 starting at day 20 and continued every second day (total of 5 drug injections) reflecting the clinical situation in which patient seeks medical help because the pain becomes significant; ii) treatment #2 starting at day 10 and continued every second day (total of 10 drug injections) aiming at establishing the disease-modifying potential of preventive treatment, when the cartilage is not yet fully degenerated. Therefore, animals in long treatment paradigm #2 were treated at day 10, 12, 14, 16, 18, 20, 22, 24, 26 and 28 after MIA administration, whereas short treatment started from day 20. A schematic representation of treatment paradigm is included in the supplementary materials. Vehicle was administered either from day 10 or 20. Pain in chronic treatment paradigm was assessed at day 21 (24 h after last treatment) and 28 (1 h after last treatment) in order to keep in line with previous results and reveal potentially long-lasting effects of the treatment. Animals were immediately returned into their home cages after treatment. The experimenters performing the behavioural tests were blinded to the treatments, and the rats were randomly assigned to each treatment group. All behavioural and biochemical experiments were performed on a group of 6 animals, Evaluations of subchondral bone morphometry were performed on a group of 5 animals. Separate sets of animals were used for each experiment. To compare novel treatment paradigm with currently available treatment strategy aimed at COX2 inhibition, NS398 was used as a reference in the acute treatment paradigm or short chronic treatment paradigm #1 to reflect clinical conditions. NS398 was chosen for the present study based on its solubility in organic solvents in order to keep the same vehicle across groups. For gene expression analysis, additional groups of sham animals receiving either vehicle of JWH133 from day 10 were used.

### 2.5. Pressure application measurement

The pressure application measurement (PAM) device (PAM; Ugo-Basile, Italy) has been used for the assessment of joint hyperalgesia [28]. A quantifiable force was applied for direct stimulation of the joint, and the automatic readout of the response was recorded. The animals were held lightly, and the operator placed a thumb with a force transducer mounted unit on one side of the animal's knee joint and a forefinger on the other. A gradually increasing squeeze force was applied across the joint at a rate of approximately 30 g/s with a maximum test duration of 15 s or applied 500 g force. Using calibrated instrumentation, the applied force in grams was displayed on a digital screen and recorded. The test end point was the point at which the animal withdrew its limb or showed any behavioural signs of discomfort or distress, such as freezing of whisker movement, wriggling or vocalizing. The peak gram force (gf) applied immediately before the limb base unit recorded withdrawal was designated as the limb withdrawal threshold (LWT), and the mean LWTs were calculated. The baseline measurements were obtained 30 min before i.p. drug administration. To compare the acute antinociceptive effects in the dose-response experiment, LWT were calculated as a maximum possible effect - %MPE = [(test LWT - baseline LWT) / maximum possible LWT - baseline LWT] x 100], which allowed us to minimise individual differences as the results were normalised to baseline measurements, i.e. increase in %MPE was proportional to baseline pain threshold of the animal allowing us to more precisely estimate acute antinociceptive effects of the given dose and make comparison. In chronic treatment paradigm, baseline measures could be affected by the treatment in the preceding days and we have only compared drug-treated group vs vehicle group with Dunnett test and therefore raw values were sufficient to assess anti-nociceptive effect at the given timepoint.

### 2.6. Kinetic weight bearing (KWB) test

To characterize pain behaviour in the MIA model, we used kinetic weight bearing (KWB), a novel instrument developed by Bioseb (France). Sensors placed on the ground measure weight borne by each individual paw during a walking sequence of a freely moving animal, while a built-in camera detects the body shape and centre of gravity of the animal, which is then used for further analysis. Rats were habituated to move through the corridor (50 × 130 cm) in few test runs for 1 week before the actual experiment. Measurements were performed at days 20, 21 and 28 following MIA administration. Data collection was terminated when 5 validated runs were obtained or after 5 min of acquisition. All collected runs for each animal were then averaged for further statistical analysis. If the animal did not run during this time window, then it was excluded from further analysis. Thus, the number of samples from KWB varied at day 28 in treatment paradigm #2. All the recorded data were then validated and refined of any noise by a blinded observer, who carefully examined video-recordings and verified that animal was not stopping during the run or that detected signal was ascribed to proper paw. The final results include information about the mean peak force and surface applied by each paw. Other data provided insight into the swing phase duration of each paw proportion of swing phase duration and the mean step duration for each paw.

### 2.7. X-ray microcomputer tomography

The *ex vivo* commercial XMT system was used (v|tome|x s, GESensing & Inspection Technologies, Phoenix|x-ray, Wunstorf, Germany). Trimmed knee samples with tibial and femur bone sections were dissected at day 28 following MIA administration and immediately stored in dry ice (−80 °C) until analysis. The samples were defrosted for 30 min prior to analysis. The XMT scanning parameters were as follows: System Phoenix v|tome|x s; voltage (kV): 200; current (μA): 110; voxel size (μm): 20; detector timing (milliseconds):131; filter Cu: 0.1. Identical scanning parameters were applied to all the samples. Each sample was placed inside the scanner chamber using the same holder, which also held the calibration phantom (QRM-MicroCT-HA D25) required for further quantitative measurements of bone mineral density (BMD). Reconstructed cross-sections were stored in 256 greyscale format (8 bits per voxel) and later processed by Drishti (open-source Volume Exploration and Presentation Tool by Limaye) to visualize the sample microstructures. The volume of interest (VOI) (15 slices x20 μm) selected from the entire stack of images was used to calculate histomorphometric parameters based on binarized images (bone volume/total volume: BV/TV, trabecular thickness: Tb.Th, and trabecular number: Tb.N) and quantitative parameters related to BMD. The data sets that were segmented using ImageJ (Wayne Rasband National Institutes of Health, USA) and processed using a self-developed plug-in to calculate the quantitative parameter hydroxyapatite density (HAD). The hydroxyapatite density was calculated using our own method for BMD measurements with the calibration curve estimated based on images of the hydroxyapatite calibration phantom scanned concurrently with the specimen, for further reference see Cyganik et al. [29].

### 2.8. RNA preparation

Cartilage and subchondral bone tissue from the medial femoral condyle was dissected on day 28 after MIA administration and 1 h after the last drug administration. Femoral condyle has been chosen for RNA measurement based on our XMT results which showed no changes in tibia morphology, however medial part was chosen based on results by Sophocleous et al., 2015, which revealed higher OARSI scoring in medial compartment of knee joints in Cnr2 / mice. The superficial part of the cartilage (3–5 mm) was harvested and placed on ice in RNA later and then stored at −80 °C. Extraction of high-quality RNA was performed according to a protocol published by Le Bleu et al., 2017.

Briefly, the tissue was placed in 500  $\mu$ L of TRIzol reagent (Invitrogen, Carlsbad, CA, USA). It was homogenized in a tissue lyser (Qiagen Inc., Hilden, Germany) at maximal frequency for a total of 5 min. Then, 500  $\mu$ L of TRIzol was added to the Eppendorf tube followed centrifugation at  $12,000 \times g$  for 5 min at  $4^\circ\text{C}$  to pellet undigested tissue. The supernatant was transferred to a new tube, and 200  $\mu$ L of chloroform was added. The sample was mixed by vigorous shaking for 30 s, allowed to stand for 3 min at room temperature, and then centrifuged at  $12,000 \times g$  for 15 min at  $4^\circ\text{C}$ . The aqueous layer was transferred to a new tube, and a mixture of concentrated sodium chloride and sodium acetate was added to achieve final concentrations of 1.2 M and 0.8 M, respectively. RNA was then precipitated by addition of 0.3 volumes of 100 % isopropanol followed by a 10-min incubation at room temperature. Centrifugation at  $12,000 \times g$  for 10 min at  $4^\circ\text{C}$  facilitated pelleting of the RNA precipitate, which was washed twice using 1 mL of 75 % (V/V) ethanol, dried for 5–10 min at  $37^\circ\text{C}$ , and re-constituted in RNase-free water. RNA was denatured for 12 min at  $65^\circ\text{C}$ . The RNA concentration was measured using a NanoDrop ND-100 Spectrometer (Thermo Scientific, Wilmington, DE, USA). The quality of the RNA was determined using a RNA 6000 Nano LabChip Kit and Agilent Bioanalyzer 2100 (Agilent, Palo Alto, CA, USA), to ensure RIN values  $\sim 9$ . Total RNA (2.5  $\mu$ g) was converted to double-stranded cDNA using iScript Reverse Transcription Supermix (Bio-Rad, Hercules, CA, USA) according to the manufacturer's protocol in a 20- $\mu$ L total volume. The complete reaction mix was incubated in a thermal cycler according to the manufacturer's protocol. cDNA was stored in  $-20^\circ\text{C}$ .

## 2.9. Quantitative polymerase chain reaction (qPCR)

The reaction was performed on Hard-Shell, thin wall PCR plate (Bio-Rad, Hercules, CA, USA, #HSP0601) with TaqMan probes and TaqMan Universal PCR Super Mix (Bio-Rad, Hercules, CA, USA) in a thermocycler C1000™ CFX96™ Real-Time system (Bio-Rad, Hercules, CA, USA) according to the manufacturer's protocol: denaturation for 30 s at  $95^\circ\text{C}$ , followed by 40 cycles of denaturation for 5 s at  $95^\circ\text{C}$ , annealing, extension and plate reading, and then 30 s at  $60^\circ\text{C}$ . 20  $\mu$ L of cDNA was diluted in 180  $\mu$ L of RNase-free water. 5.5  $\mu$ L of cDNA solution was added to 4.5  $\mu$ L of TaqMan Universal PCR Super Mix working solution. Samples were run in duplicates. The threshold cycle (CT) value (cycle during which the fluorescence exceeds the threshold value) for each gene was normalized to the CT value of the beta-2 microglobulin (*B2m*) reference gene, which was selected upon literature findings [30,31]. RNA abundance was calculated as  $2^{-\Delta\text{CT}}$  (normalized  $\Delta\text{CT}$ ). The results are presented as the fold change proportional to the expression level in sham vehicle-treated animals. The following assays (TaqMan Gene Expression Assays, Life Technologies, USA) were used in the experiment: Rn00560865 (*B2m*), Rn01762845\_m1 (*Adamts14*), Rn01538170\_m1 (*Mmp2*), Rn00579162\_m1 (*Mmp9*), Rn01430873\_g1 (*Timp1*), Rn00563255\_m1 (*Comp*), Rn01439585\_m1 (*Col15a1*), Rn01489555\_m1 (*Col4a3bp*), Rn01536936\_g1 (*Ccl17*), Rn01432377\_m1 (*Il34*), Rn00580555\_m1 (*Ccl2*), Rn01410330\_m1 (*Il6*), Rn00577366\_m1 (*Fabp3*).

## 2.10. Statistical analysis

The analysis was performed using Prism V.5 (GraphPad Software). Changes in the limb withdrawal threshold throughout the time-course were analysed using two-way analysis of variance with a Bonferroni post hoc test. Kinetic weight bearing data were analysed using one-way analysis of variance with the Bonferroni multiple comparison test for rear paws in the respective treatment groups. XMT data were analysed by one-way analysis of variance with Dunnett's post-hoc test for comparison of treatment effects with the vehicle group. Post-hoc analysis was performed only if the F was significant and there was no variance inhomogeneity. The number of animals used in the study was calculated *a priori* using power analysis and the pwr package in R. The effect size

$f=1$  was calculated from previous data assuming the desired power = 0.9. The number of animals used in the treatment groups was  $N = 6$ , excluding the XMT experiment, in which it was  $N = 5$ . Additionally, in the prolonged treatment experiment in PAM, there were two vehicle groups, starting from day 10 and day 20, with  $N = 5$ . There was no significant difference between the two vehicle groups, so they were pooled from day 20 ( $N = 10$ ). We did not involve sham group in behavioural experiments as the MIA model is well established and we have published few paper already within this model [19,26,27,32,33] in order to reduce the number of animals. However, sham group was involved in the biochemical assessment in order to see if JWH133 is influencing healthy animals. All the data were normally distributed, and no inhomogeneity of variances was detected by Bartlett's test. The data were considered significant only when  $P \leq 0.05$ . All data analyses were performed under blinded conditions.

## 3. Results

### 3.1. Antinociceptive dose-response effects of CB2 agonists in the acute treatment paradigm

An acute nociceptive effect of CB2 agonists was established by measuring knee hypersensitivity with PAM (Fig. 1). GW833972A at doses of 1 mg/kg did not produce statistically significant mechanical antinociception at any time point measured. JWH133 at a dose of 1 mg/kg produced analgesic effects from 60 min to 120 min post i.p. administration. The 5 mg/kg of GW833972A produced analgesic effects from 60 min to 120 min post i.p. administration. The effects of GW833972A at 5 mg/kg and JWH133 at 1 mg/kg were not significantly different throughout the course of the experiment; however, both JWH133 (1 mg/kg) and GW833972A (5 mg/kg) elicited a significantly stronger analgesic effect than 1 mg/kg of GW833972A at 60 min. Therefore, doses of 1 mg/kg of JWH133 and 5 mg/kg of GW833972A were selected for further experiments.

In the KWB test, we measured the ability of acute CB2 agonist treatment to reverse OA-induced weight bearing impairment. The test was performed at day 21 post MIA injection, 1 h after i.p. administration of either vehicle or CB2 agonists: JWH133 or GW833972A. In the vehicle group, we observed significant loss of symmetry in weight bearing, as measured by the peak force, peak surface, swing duration and laid/duration applied by rear paws when the rat walked through the corridor (Fig. 2A–D). However, disarrangement of all the weight bearing parameters was reversed by i.p. administration of both CB2 agonists,

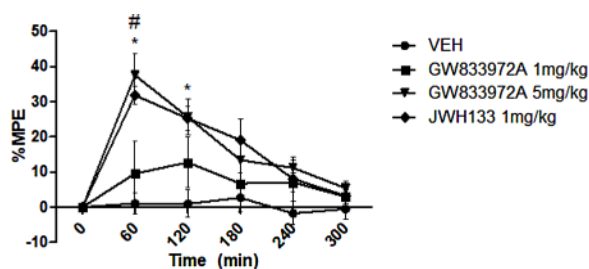


**Fig. 1.** Antinociceptive effects of acute, systemic administration of CB2 agonists (JWH133 and GW833972A) on knee joint hypersensitivity in OA rats. The pressure application measurement (PAM) test was performed at day 28 post MIA i.a. injection and 1 h post i.p. drug administration (i.p.): JWH133 (1 mg/kg), GW833972A (1 mg/kg and 5 mg/kg) or Vehicle (VEH). The hind limb knee withdrawal threshold was assessed during a 300-min period. Results are presented as means of the maximum possible effect percentage (% MPE)  $\pm$  SEM with  $N = 6$  for each experimental group. Statistical analysis was performed using two-way ANOVA followed by the Bonferroni post hoc test with a  $p \leq 0.05$  confidence interval. \*Denotes significance between the VEH and pharmacological treatment groups at the same time point, # denotes significance between the GW833972A (1 mg/kg) and other groups at the same time point.

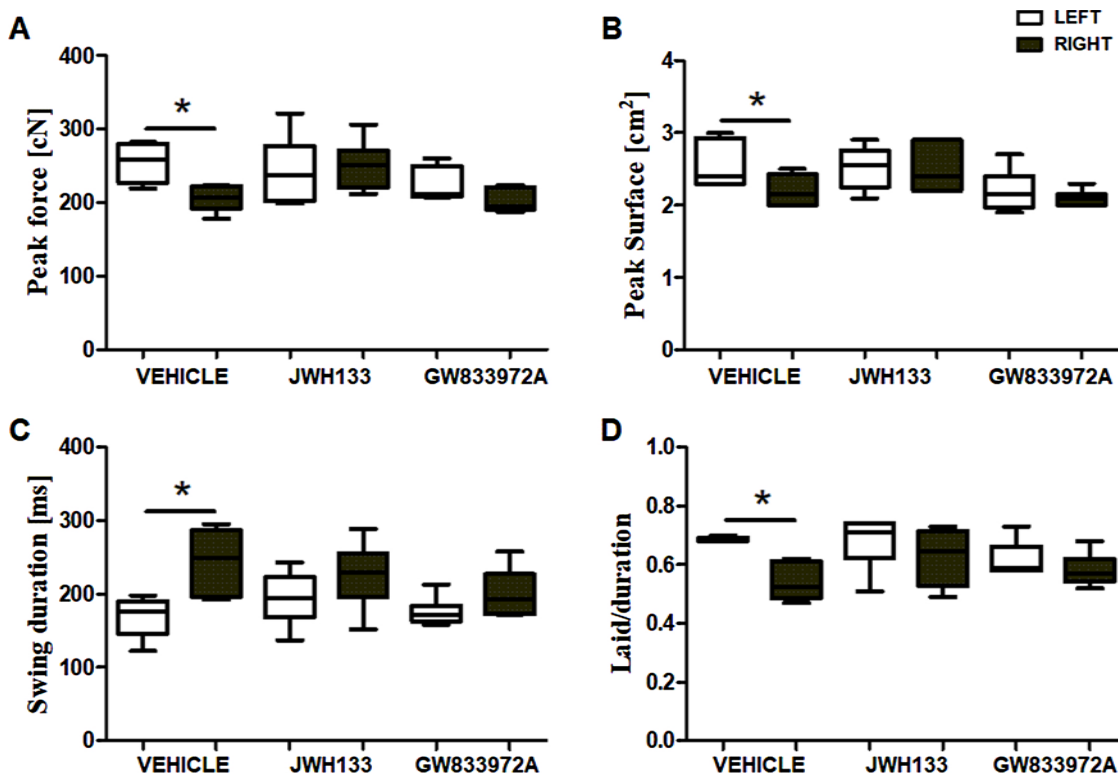


**Fig. 2.** Effects of acute systemic administration of CB2 agonists (JWH133 and GW933972A) on the kinetic weight bearing (KWB) test in osteoarthritic rats. Gait analysis was performed on day 21 after MIA injection (i.a.) and 1 h after drug administration (i.p.): JWH-133 (1 mg/kg), GW933972A (5 mg/kg) or Vehicle. Data are presented as means  $\pm$  min to max for peak force (A), peak surface (B), swing duration (C), and laid/duration (D) of the rear left (healthy hind limb, white square) and rear right (OA hind limb, dark grey square). Statistical analysis was performed using one-way ANOVA followed by Bonferroni post hoc test with a  $p < 0.05$  confidence interval. Each experimental group included  $N = 6$  rats. \*Denotes significant differences between the rear left vs rear right paws in each group.

JWH133 and GW833972A at doses of 1 mg/kg and 5 mg/kg, respectively (Fig. 2A–D).

**3.2. Antinociceptive effects of CB2 agonists in the chronic treatment paradigm**

Chronic treatment paradigm #2 starting from day 10 post OA-induction for 1 mg/kg of JWH133 caused a significant increase in paw

withdrawal force in PAM starting as early as day 12 and all subsequent time-points tested, whereas chronic treatment paradigm #1 starting from day 20 with 1 mg/kg of JWH133 elicited an increase in paw withdrawal force throughout the course of the experiment (Fig. 3). Chronic treatment paradigm #2 starting from day 10 with 5 mg/kg of GW833972A caused a significant increase in paw withdrawal force in PAM only at day 12 and 14 and then steadily declined, whereas chronic treatment paradigm #1 starting from day 20 with 5 mg/kg of

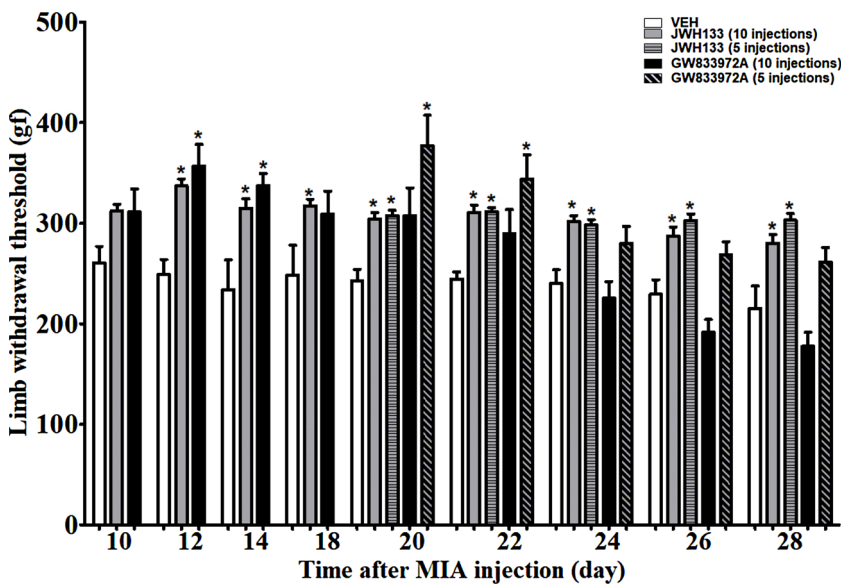


**Fig. 3.** Antinociceptive effects of CB2 agonists on knee joint hypersensitivity upon two different chronic drug administration schemes in osteoarthritic rats. Compounds JWH133 (1 mg/kg) and GW933972A (5 mg/kg) or Vehicle (VEH) were evaluated. The pressure application measurement (PAM) test was performed each second day 1 h after drug administration (i.p.) starting from day 10 up to day 28 (treatment paradigm #2, 10 injections) or beginning from day 20 (treatment paradigm #1, 5 injections). Data are presented as means of the limb withdrawal threshold (gf)  $\pm$  SEM from a group of  $n = 5-10$  animals. Statistical analysis was performed using two-way ANOVA followed by Bonferroni post-hoc test with  $p < 0.05$  confidence intervals. \*Denotes significance vs. vehicle at the same time point (day).

GW833972A elicited an increase in the paw withdrawal threshold at day 20 and 22 (Fig. 3). In KWB, we observed full restoration of gait parameters following JWH133 (1 mg/kg) treatment from day 10 to day 21, but no effects of JWH133 (1 mg/kg) treatment from day 20 (Fig. 4A–D). Conversely, GW833972A (5 mg/kg) treatment paradigm #2 starting from day 10 had no effects on peak force and surface at day 21 (Fig. 4A–B), but it did restore the disproportion in swing duration and laid/duration at this timepoint (Fig. 4C–D). GW833972A (5 mg/kg) given in treatment paradigm #1 starting from day 20 was able to restore gait parameters at day 21 (Fig. 4A–D). At day 28, we observed no effects of GW833972A (5 mg/kg) on gait parameters in any treatment regimen (Fig. 5A–D). JWH133 (1 mg/kg) in both treatment regimens was able to rebalance the peak surface applied by the rear paws at day 28 (Fig. 5B), but it did not affect other gait parameters (Fig. 5A, C–D).

### 3.3. Antinociceptive effects of NS398, COX2 inhibitor in the chronic treatment paradigm

Behavioural assessment of the prolonged analgesic potential of NS398, COX2 inhibitor was performed to compare it with the therapeutic potential of CB2 agonists. NS398 was used in short treatment paradigm #1. Similarly to CB2 agonists, acute administration of NS398 was able to restore symmetry in weight bearing parameters in the KWB test (Fig. 6A–D) 1 h after i.p. administration at day 20. Albeit, in the chronic treatment paradigm, we did not observe any improvement of the impaired weight bearing in KWB on either day 21 (Fig. 6E–H) or 28 (Fig. 6I–M).

### 3.4. Morphometric analysis of femur s subchondral bone tissue following JWH133 treatment by X-ray microtomography

Based on behavioural data, JWH133 was selected for further experiments upon disease-modifying properties. X-ray microtomography of femur subchondral bone tissue revealed an increase in bone mineral density (BMD, Fig. 7A) and bone volume fraction (BV/TV, Fig. 7B) but a decrease in trabecular spacing (Tb.Sp, Fig. 7C) at day 28 following chronic pharmacological treatment with NS398, a COX2 inhibitor (paradigm #1), and JWH133, a CB2 agonist (both in paradigm #1 and #2). Trabecular thickness (Tb.Th, Fig. 7D) was not affected by either drug. Fig. 7E shows representative samples.

### 3.5. Changes in gene expression in the cartilage and subchondral bone following CB2 agonist treatment

Gene expression analysis in the cartilage and subchondral bone was performed to evaluate the molecular mechanisms underlying tissue remodelling effects of JWH133 in the MIA model of OA. Genes were initially preselected based on the RNAseq results (Table and heatmap in supplementary materials), however some additional targets were also taken under consideration. RT-qPCR analysis revealed a significant increase in the expression of mRNA encoding peptidases involved in the degradation and building of extracellular matrix, namely *Adamtsl4*, *Mmp2*, *Mmp9*, *Timp1*, *Comp* and *Col15a1* (Fig. 8A–F), in OA cartilage in comparison to sham treated animals (MIA vs NaCl). In contrast, the *Col4a3bp* gene encoding ceramide transfer protein was decreased in OA cartilage (Fig. 8G). Moreover, expression of mRNA encoding chemoattractant (*Ccl2* and *Ccl17*) and proinflammatory (*Il6*, *Il34*) proteins were also upregulated in OA cartilage (Fig. 8H–K, MIA vs NaCl). Gene expression of the extracellular matrix proteins *Mmp2*, *Mmp9*, *Timp1*,

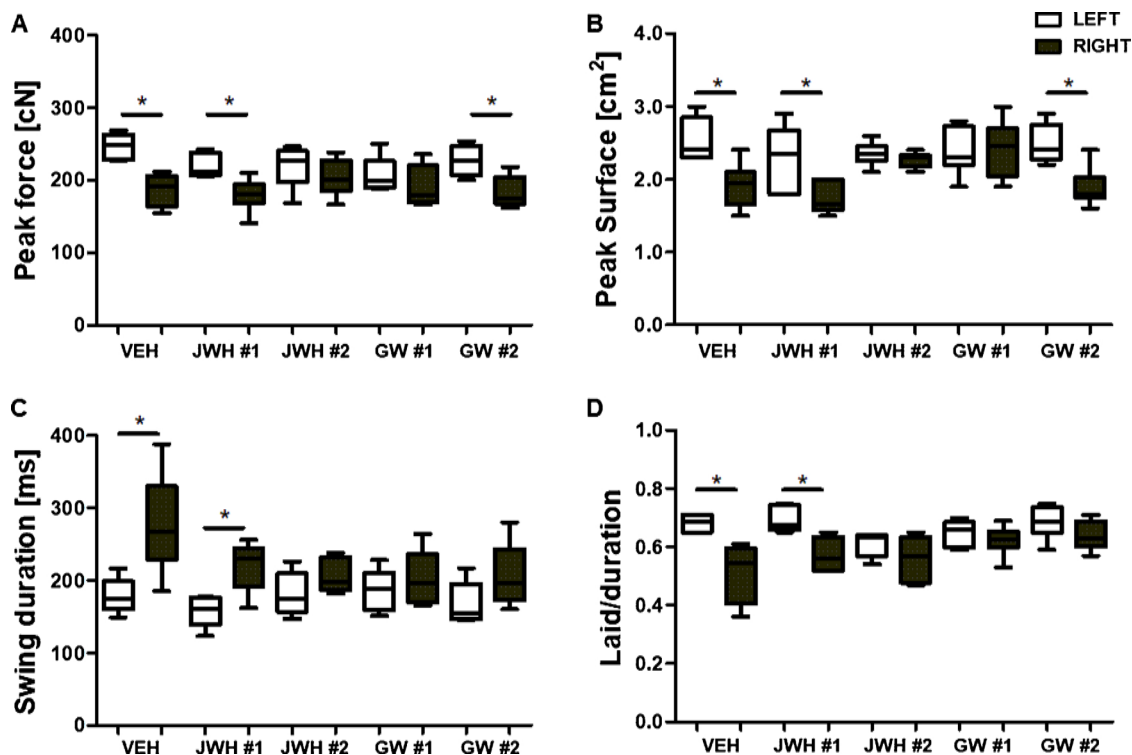
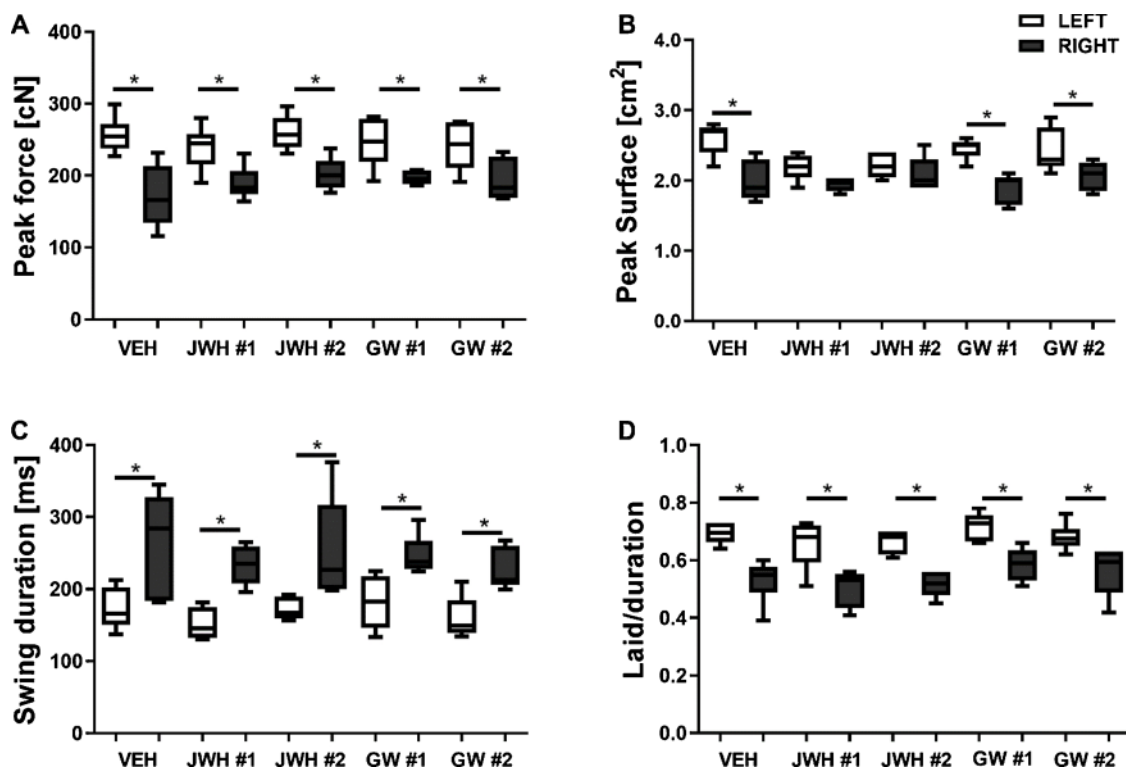


Fig. 4. Gait analysis at day 21 in osteoarthritic rats following vehicle or CB2 agonists: JWH133 (JWH) or GW933972A (GW) injection in two treatment paradigms. Experiments were performed 24 h post drug i.p. administration at day 21 after MIA injection. Rats were treated with JWH133 (1 mg/kg), GW933972A (5 mg/kg) or Vehicle (VEH) in two chronic schemes : Treatment scheme 1 (#1, from day 20th to 28th) or Treatment scheme 2 (#2 from day 10th to 28th). Data are presented as means  $\pm$  min to max for peak force (A), peak surface (B), swing duration (C), and laid/duration (D) of rear left (healthy hind limb, white square) and rear right (OA hind limb, dark grey square). Statistical analysis was performed using one-way ANOVA followed by Bonferroni post hoc test with  $p < 0.05$  confidence interval. Each experimental group includes  $N = 6$  rats. \*Denotes significant differences rear left vs rear right paws in each group.



**Fig. 5.** Gait analysis at day 28 in osteoarthritic rats following vehicle or CB2 agonists: JWH133 (JWH) or GW933972A (GW) injection in two treatment paradigms. Experiments were performed 24 h post drug i.p. administration at day 21 post MIA injection. Rats were treated with JWH133 (1 mg/kg), GW933972A (5 mg/kg) or Vehicle (VEH) in two chronic schemes: Treatment paradigm 1 (#1, from day 20 to 28) or Treatment paradigm 2 (#2 from day 10 to 28). Data are presented as means  $\pm$  min to max for peak force (A), peak surface (B), swing duration (C), and laid/duration (D) of rear left (healthy hind limb, white square) and rear right (OA hind limb, dark grey square). Statistical analysis was performed using one-way ANOVA followed by the Bonferroni post hoc test with  $p < 0.05$  confidence intervals. Each experimental group included  $N = 6$  rats. \*Denotes significant differences rear left vs rear right paws in each group.

*Comp*, *Col15a1* and proinflammatory factors, *Ccl17* and *Il34* was significantly lower in the MIA group following JWH133 treatment from day 10 in comparison to the vehicle-treated group (Fig. 8A–F). Additionally, JWH133 treatment from day 10 reversed changes in expression of *Col4a3bp*, *Ccl2* and *Il6* (Fig. 8G, J–K) to a level that was no longer significantly different from their expression pattern in sham-operated animals. Interestingly, there was also a significant increase in *Fabp3* expression in OA tissue (MIA vs NaCl), which was significantly decreased following JWH133 treatment (Fig. 8L, MIA/VEH vs MIA/JWH133). It is noteworthy to mention that JWH133 treatment did not influence the expression of tissue remodelling nor inflammatory factors in the sham-operated animals.

#### 4. Conclusions

The present behavioural data revealed acute and prolonged antinociceptive effects of a cAMP-biased CB2 agonist, JWH133. In contrast, the analgesic potential of a  $\beta$ -arrestin-biased CB2 agonist, GW833972A, was hampered due to rapid and pronounced tolerance development. These results reveal that  $\beta$ -arrestin recruitment is a significant molecular factor underlying tolerance development toward the analgesic properties of cannabinoids. The role of  $\beta$ -arrestin recruitment in analgesic tolerance development has been revealed in several studies [34]; however, to the best of our knowledge, this is the first study to elucidate a significant discrepancy in tolerance development between two functionally biased agonists. The results of this study contribute to the improvement of drug-design processes for novel analgesics, including both cannabinoid and potentially opioid drugs.

Previously, our group has shown a marked increase in MMPs and CB2 expression in an animal model of OA [35]. We have also obtained promising data with dual FAAH inhibitor and TRPV1 antagonist,

OMDM198, which elicited effective analgesia in MIA model of OA [27] and decreased expression of molecular factors possibly underlying the neuropathic component of OA related pain [32], suggesting beneficial effects of increased endocannabinoid tone in OA. Research led by other authors have revealed that a mixed CB1 and CB2 agonist, WIN55,212-2, is able to decrease expression of *Mmp3* and *Mmp13* in chondrocytes *in vitro* [22]. Moreover, deletion of CB2 has been shown to intensify lesions in a surgical model of OA in mice and decrease proteoglycan production in chondrocytes *in vitro* [21]. Acute administration of CB2 agonist is able to exert both analgesia and reverse the anxiogenic phenotype related to OA in mice [36]. Conversely, CB2 overexpression is able to counteract allodynia development in a mouse model of OA [37], and chronic CB2 agonist treatment is able to reduce lesions in a surgical model of OA [21]. Furthermore, various studies have provided compelling evidence regarding functional role of CB2 receptors in bone tissue. Offek et al. have shown both CB2 expression in osteoblasts, osteocytes, and osteoclasts [38]. CB2-deficient mice are characterized by age-related trabecular bone loss [38] high-turnover osteoporosis with relative uncoupling of bone resorption from bone formation [39]. Treatment with the sustained CB2 agonist HU308 showed partial protection against ovariectomy-induced bone loss in wild-type mice *in vivo* [39].

Our results add to these findings regarding the molecular underpinnings of the analgesic and disease-modifying properties of CB2 agonism in a chemically induced model of OA in rats, with a particular interest in drug selection based on the molecular properties. Our data revealed both analgesic and disease-modifying properties of the CB2 agonist JWH133 in a wide battery of assays. Improvement in subchondral bone tissue morphology in the  $\mu$ CT analysis was supported by downregulation of MMPs following JWH133 treatment. Moreover, JWH133 was able to decrease gene expression of inflammatory factors, namely *Ccl2*, *Ccl17*, *Il34* and *Il6*, in OA cartilage, supporting its plausible

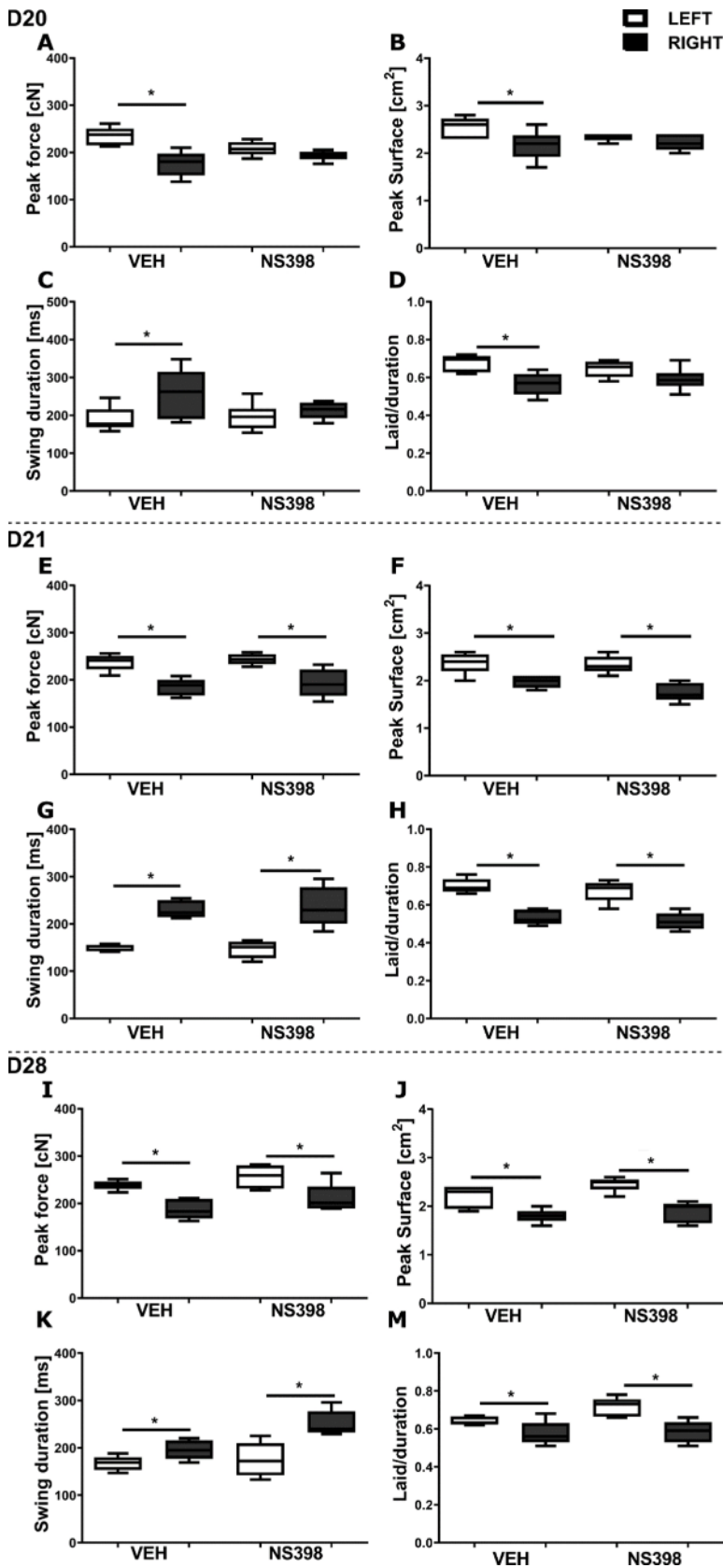


**Fig. 6.** Effect of acute and chronic COX2 inhibitor NS398 (5 mg/kg) administration on kinetic weight bearing (KWB) in osteoarthritic rats. Gait analysis was performed at day 20 and 28 1 h post i.p. drug administration (A–D; IM–), whereas gait analysis at day 21 was performed 24 h post drugs i.p. administration (E–H). Data are presented as means  $\pm$  min to max from a group (A, I) peak surface (B, J), swing duration (C, K), and laid/duration (D, M) of rear left (healthy hind limb, white square) and rear right (OA hind limb, dark grey square). Statistical analysis was performed using one-way ANOVA followed by Bonferroni post hoc test with  $p < 0.05$  confidence intervals. Each experimental group includes  $N = 5$  rats. \*Denotes significant differences rear left vs rear right paws in each group.

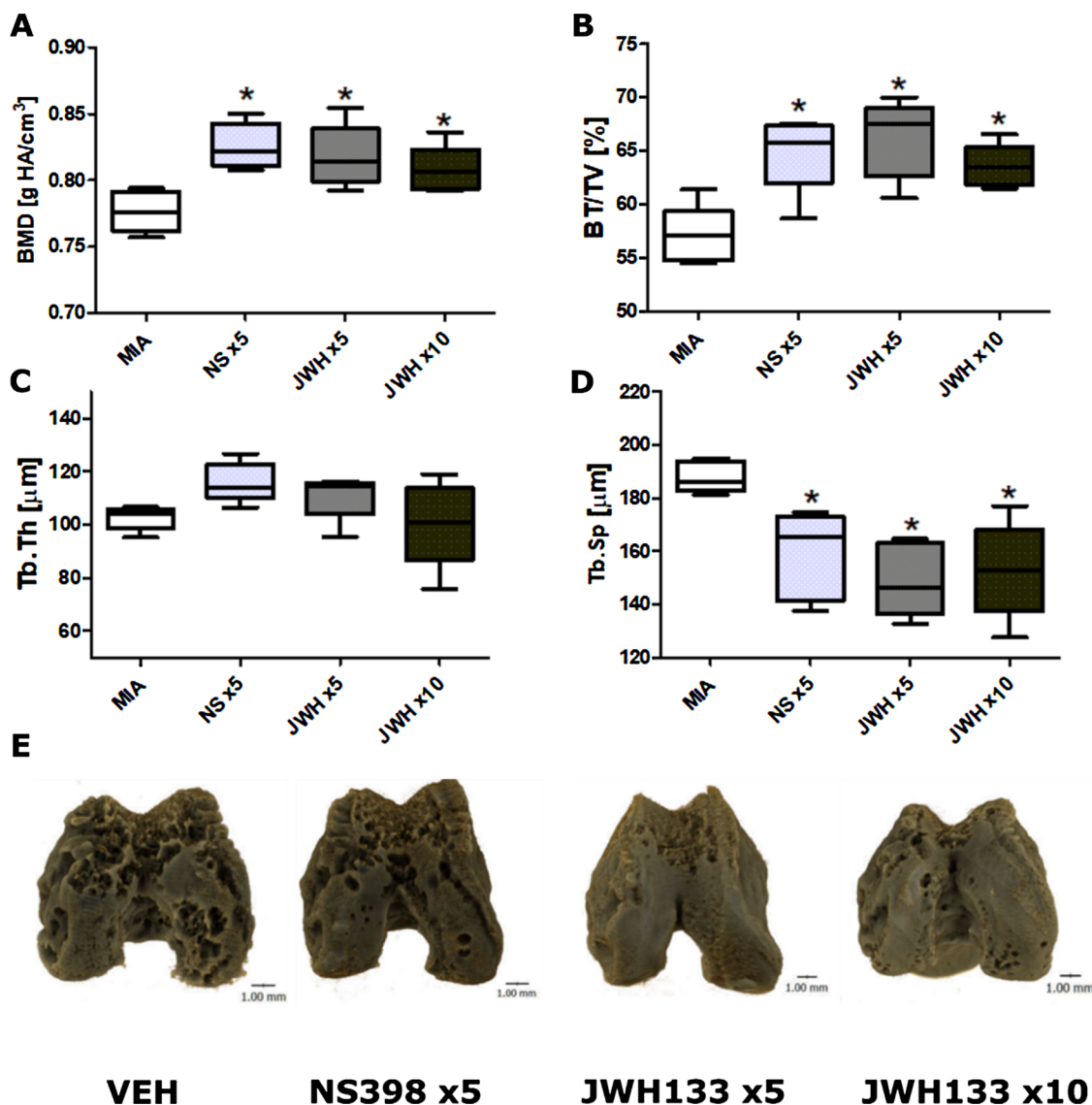


**Fig. 7.** Effect of NS398 and JWH-133 chronic administration on femoral subchondral bone properties in osteoarthritic rats. Morphometric analysis (A–D) with 3-dimensional visualization (E) was performed at day 28 post MIA injection in animals receiving repeated treatments (i.p.) with 5 mg/kg of NS398 (treatment paradigm #1, 5 injections, from day 20th to 28th), 1 mg/kg JWH-133 (treatment paradigm #1, 5 injections, from day 20th to 28th and treatment paradigm #2, 10 injections, from day 10th to 28th) or Vehicle (VEH). Data are presented as unit means ± SEM for (A) bone mineral density (BMD), (B) bone volume (BT/TV) (C) trabecular thickness (Tb.Th), (D) trabecular spacing (Tb.Sp). Statistical analysis was performed using one-way ANOVA followed by Dunnett’s post hoc test with p 0.05 confidence interval. Each experimental group includes n = 5 rats. \*Denotes significant differences against VEH.

mechanism of action. Indeed, several studies have shown that pro-inflammatory cytokines such as IL6 and CCL2 induce the expression of MMPs in cartilage [5,6]. Similarly, there is a positive correlation between IL6 and MMPs levels in cartilage [40] and synovial fluid of OA patients, which is also related to severe radiographic changes [5].

Despite the well documented role of MMPs in OA development and the protective effects of their inhibition [41,42], broad-spectrum MMPs inhibitors have failed in clinical trials, at least in part due to a painful, joint-stiffening side effect, termed musculoskeletal syndrome [43], probably as a result of insufficient selectivity toward specific MMPs [44]. CB2 agonists may provide a safe treatment strategy to decrease MMPs expression in OA cartilage without targeting MMPs production in healthy tissue, as seen in our experiment in sham-treated animals. Moreover, CCL2, CCL17 and IL6 inhibition were shown to be protective in an animal model of OA [45–48]. It is plausible to suspect that the protective effects of CB2 agonist on the knee sample morphology and MMPs expression in the present study was interlinked with the anti-inflammatory properties of cannabinoids.

We also compared the analgesic and disease-modifying properties with a currently available treatment strategy – COX2 inhibition. COX2 inhibitors are widely used for their analgesic action; however, little is known about their impact on bone physiology. In fact, the COX2 metabolic product, prostaglandin E2, can stimulate the differentiation of both osteoblasts and osteoclasts [49]. COX2 inhibition has been shown to impair bone healing following fracture [50,51]. In our study, the COX2 inhibitor NS398 was able to improve the subchondral bone morphology during OA development, but it failed to induce significant analgesia in the chronic treatment paradigm. In clinical conditions, nearly 40 % of patients do not respond to treatment with COX2 inhibitors [52], which could be related to the neuropathic component of pain mediated by central sensitization phenomenon that occurs in one-third of patients [53]. We have previously reported that cannabinoids are able to counteract central sensitization in an animal model of OA at a molecular level [32]. This phenomenon could explain the superior analgesic potential of CB2 agonists compared with the COX2 inhibitor NS398, despite their similar effects on the subchondral bone

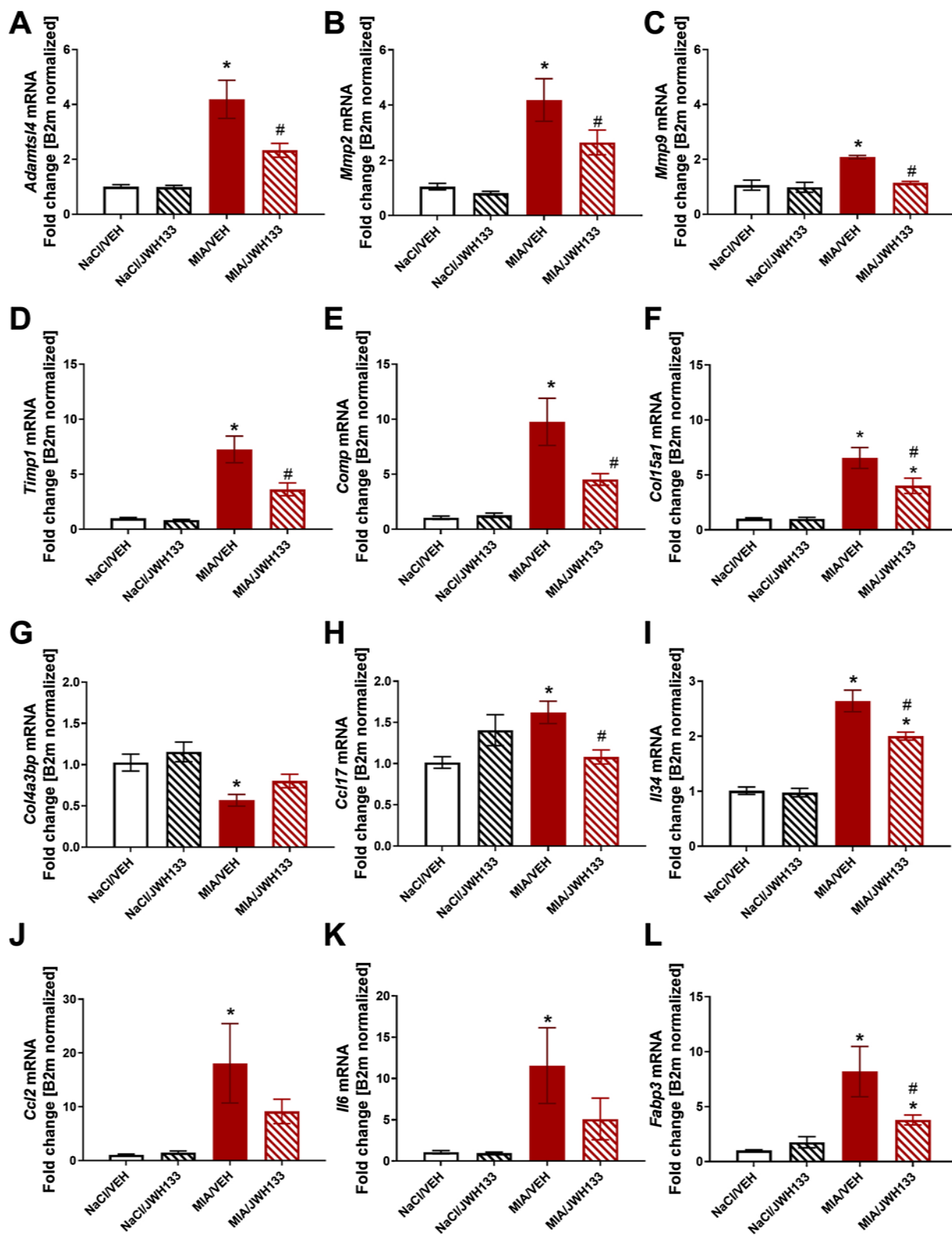


**Fig. 8.** Effect of JWH-133 systemic and repeated administration on cartilage molecular markers in healthy and osteoarthritic rats. Gene expression (qPCR analysis) of selected molecules was evaluated in cartilage tissue at day 28 post MIA (OA) or NaCl (SHAM) (i.a.) injection. Treatment with 1 mg/kg JWH-133 (scheme #2, 10 injections, from day 10 to 28) or Vehicle (VEH) was performed in both OA and SHAM rats. Data are presented as the mean  $\pm$  SEM of fold change normalized to reference gene, beta-2 microglobulin (*B2m*). Statistical analysis was performed using one-way ANOVA followed by Tukey post hoc test with  $p < 0.05$  confidence interval. Each experimental group includes  $n = 6$  rats. \*Denotes significant differences vs. NaCl/Veh; #Denotes significant differences vs. MIA/VEH.

morphology. Conflicting results with prior findings about impaired bone healing due to COX2 inhibition may be explained by differences in the source of damage. In the case of OA, instead of a rather mechanical insult, the biochemical disturbances in subchondral bone and cartilage are thought to be the major cause of tissue breakdown. Moreover, Gruber et al. have shown that COX2 activity is necessary for osteoclast-like cell formation, and therefore, COX2 inhibition may promote maintenance of healthy subchondral bone architecture during OA progression [54]. However, the role of COX2 enzyme in OA cartilage and bone requires further study.

Moreover, this and previous studies by our group and others have revealed multiple changes in gene expression patterns in a MIA model of OA, which are in agreement with clinical findings regarding genes associated with OA development, namely the upregulation of MMPs [35], *Col15a1* [55], IL34 [56,57] and COMP [58,59], presenting the MIA model as relatively reliable animal model of OA. The data presented herein add to these findings concerning the expression changes in *Col4a3bp*, *Adatmsl4* and *Fabp3*. The upregulation of *Fabp3* (8-fold increase in the MIA group vs Sham-treated animals) is of particular interest in relation to the endocannabinoid system and inflammation, as FABP3 is involved in arachidonic acid metabolism [60], and little is known about its role in cartilage [61].

It is important to note some limitations of this study. First, it is not known whether the favourable molecular changes following JWH133 are directly related to CB2 agonism or are merely a consequence of protection against cartilage and subchondral bone destruction. It would be reasonable to perform additional experiments using the CB2 antagonist, which was not used herein due to the large-scale experiments. Our focus rather was on different aspects of CB2-aimed therapeutic properties, such as a comparison of effects between various treatment strategies in the prolonged treatment paradigm. Moreover, the compounds used herein are considered to be specific [62], and therefore, off-target effects may be presumed to be excluded from the current study. However, it must be noted that presented results concern animal model of OA, which may vary in both etiology and pathophysiology from human OA. For example, MIA induced apoptosis is non-selective and affects all cell types within the knee joint, it is plausible that the nerve damage and pain phenotype observed in this model is a direct result of MIA injection [63], rather than a consequence of cartilage degeneration. Further studies with either CB2 antagonists, novel pharmacological tools (FABPs inhibitors for example) or modulators of intracellular effector pathways are required to establish the precise mechanism of action of CB2 agonists and the endocannabinoid system in the pathophysiology of OA.

In conclusion, our data not only show the analgesic potential of CB2 agonists in OA treatment but also reveal its disease-modifying potential supported by molecular underpinnings. Although, one must consider that the etiology and anatomy of human OA is much different from the MIA model in rats. Therefore, CB2 agonists should be researched in bigger species and models with higher translational value to validate their therapeutic potential for human OA. Fortunately, experiments performed within our study are also important in the wider context of drug development based on GPCR agonists. Functional selectivity towards intracellular downstream pathways is relevant to the observable effects *in vivo*, as observed by the more pronounced tolerance development toward the analgesic effects of GW833972A. Therefore, these findings should improve the selection process of successful drug-candidate for more capital- and labour-intensive research. Despite the limitations of this study, results from our group and other authors [21, 64] hold promise for the development of efficient CB2-aimed analgesic therapy for OA that would also be able to slow down disease progression.

#### Declaration of Competing Interest

The authors declare that they have no known competing financial interests or personal relationships that could have appeared to influence

the work reported in this paper.

#### Acknowledgements

This study was financially supported through a grant from the Polish National Science Centre Grant no. OPUS no. 2014/13/B/NZ7/02311, 2015-2018 and statutory funds from the Maj Institute of PAS, Krakow, Poland. Open access publishing of this article was funded by the Ministry of Science and Higher Education, Poland under the agreement No. 879/P-DUN/2019.

#### Appendix A. Supplementary data

Supplementary material related to this article can be found, in the online version, at doi:<https://doi.org/10.1016/j.biopha.2021.111283>.

#### References

- [1] A. Haseeb, T.M. Haqqi, Immunopathogenesis of osteoarthritis, *Clin. Immunol.* 146 (2013) 185–196, <https://doi.org/10.1016/j.clim.2012.12.011>.
- [2] M. Cross, E. Smith, D. Hoy, S. Nolte, I. Ackerman, M. Fransen, L. Bridgett, S. Williams, F. Guillemin, C.L. Hill, L.L. Laslett, G. Jones, F. Cicuttini, R. Osborne, T. Vos, R. Buchbinder, A. Woolf, L. March, The global burden of hip and knee osteoarthritis: Estimates from the Global Burden of Disease 2010 study, *Ann. Rheum. Dis.* 73 (2014) 1323–1330, <https://doi.org/10.1136/annrheumdis-2013-204763>.
- [3] H. Birkedal-Hansen, Proteolytic remodeling of extracellular matrix, *Curr. Opin. Cell Biol.* 7 (5) (1995) 728–735, [https://doi.org/10.1016/0955-0674\(95\)80116-2](https://doi.org/10.1016/0955-0674(95)80116-2).
- [4] G.Q. Zeng, A.B. Chen, W. Li, J.H. Song, C.Y. Gao, High MMP-1, MMP-2, and MMP-9 protein levels in osteoarthritis, *Genet. Mol. Res.* 14 (4) (2015) 14811–14822, <https://doi.org/10.4238/2015.November.18.46>.
- [5] K. Vuolteenaho, A. Koskinen-Kolasa, M. Laavola, R. Nieminen, T. Moilanen, E. Moilanen, High synovial fluid interleukin-6 levels are associated with increased matrix metalloproteinase levels and severe radiographic changes in osteoarthritis patients, *Osteoarthr. Cartil.* 25 (1) (2017) 92–93, <https://doi.org/10.1016/j.joca.2017.02.147>.
- [6] Y.K. Xu, Y. Ke, B. Wang, J.H. Lin, The role of MCP-1-CCR2 ligand-receptor axis in chondrocyte degradation and disease progress in knee osteoarthritis, *Biol. Res.* 48 (2015), 64, <https://doi.org/10.1186/s40659-015-0057-0>.
- [7] J.D. Johnston, W.D. Burnett, S.A. Kontulainen, Subchondral Bone Features and Mechanical Properties as Biomarkers of Osteoarthritis, Springer, Dordrecht, 2016, pp. 1–27, [https://doi.org/10.1007/978-94-007-7745-3\\_46-1](https://doi.org/10.1007/978-94-007-7745-3_46-1).
- [8] S. Zhu, J. Zhu, G. Zhen, Y. Hu, S. An, Y. Li, Q. Zheng, Z. Chen, Y. Yang, M. Wan, R. L. Skolasky, Y. Cao, T. Wu, B. Gao, M. Yang, M. Gao, J. Kuliwaba, S. Ni, L. Wang, C. Wu, D. Findlay, H.K. Eltzschig, H.W. Ouyang, J. Crane, F.Q. Zhou, Y. Guan, X. Dong, X. Cao, Subchondral bone osteoclasts induce sensory innervation and osteoarthritis pain, *J. Clin. Invest.* 129 (2019) 1076–1093, <https://doi.org/10.1172/JCI121561>.
- [9] D.S. Amarasekara, H. Yun, S. Kim, N. Lee, H. Kim, J. Rho, Regulation of osteoclast differentiation by cytokine networks, *Immune Netw.* 18 (2018), <https://doi.org/10.4110/in.2018.18.e8>.
- [10] H. Löfvall, H. Newbould, M.A. Karsdal, M.H. Dziogiel, J. Richter, K. Henriksen, C. S. Thudium, Osteoclasts degrade bone and cartilage knee joint compartments through different resorption processes, *Arthritis Res. Ther.* 20 (2018) 67, <https://doi.org/10.1186/s13075-018-1564-5>.
- [11] A. Bertuglia, M. Lacourt, C. Girard, G. Beauchamp, H. Richard, S. Laverty, Osteoclasts are recruited to the subchondral bone in naturally occurring post-traumatic equine carpal osteoarthritis and may contribute to cartilage degradation, *Osteoarthr. Cartil.* 24 (2016) 555–566, <https://doi.org/10.1016/j.joca.2015.10.008>.
- [12] A. Pilichou, I. Papassotiropoulos, K. Michalakakou, S. Fessatou, E. Fandridis, G. Papachristou, E. Terpos, High levels of synovial fluid osteoprotegerin (OPG) and increased serum ratio of receptor activator of nuclear factor- $\kappa$ B ligand (RANKL) to OPG correlate with disease severity in patients with primary knee osteoarthritis, *Clin. Biochem.* 41 (2008) 746–749, <https://doi.org/10.1016/j.clinbiochem.2008.02.011>.
- [13] A. van Walsem, S. Pandhi, R.M. Nixon, P. Guyot, A. Karabis, R.A. Moore, Relative benefit-risk comparing diclofenac to other traditional non-steroidal anti-inflammatory drugs and cyclooxygenase-2 inhibitors in patients with osteoarthritis or rheumatoid arthritis: a network meta-analysis, *Arthritis Res. Ther.* 17 (2015) 66, <https://doi.org/10.1186/s13075-015-0554-0>.
- [14] R.G. Pertwee, Cannabinoid pharmacology: the first 66 years, *Br. J. Pharmacol.* 147 (2009) S163–S171, <https://doi.org/10.1038/sj.bjp.0706406>.
- [15] D. Bridges, K. Ahmad, A.S.C. Rice, The synthetic cannabinoid WIN55,212-2 attenuates hyperalgesia and allodynia in a rat model of neuropathic pain, *Br. J. Pharmacol.* 133 (2001) 586–594, <https://doi.org/10.1038/sj.bjp.0704110>.
- [16] N. Schuelert, J.J. McDougall, Cannabinoid-mediated antinociception is enhanced in rat osteoarthritic knees, *Arthritis Rheum.* 58 (2008) 145–153, <https://doi.org/10.1002/art.23156>.
- [17] N. Schuelert, M.P. Johnson, J.L. Oskins, K. Jassal, M.G. Chambers, J.J. McDougall, Local application of the endocannabinoid hydrolysis inhibitor URB597 reduces

- nociception in spontaneous and chemically induced models of osteoarthritis, *Pain* 152 (2011) 975–981, <https://doi.org/10.1016/j.pain.2010.11.025>.
- [18] I. Danovitch, D.A. Gorelick, State of the art treatments for cannabis dependence, *Psychiatr. Clin. North Am.* 35 (2012) 309–326, <https://doi.org/10.1016/j.psc.2012.03.003>.
- [19] C. Mugnaini, M. Kostrzewa, M. Bryk, A.M. Mahmoud, A. Brizzi, S. Lamponi, G. Giorgi, F. Ferlenghi, F. Vacondio, P. Maccioni, G. Colombo, M. Mor, K. Starowicz, V. Di Marzo, A. Ligresti, F. Corelli, Design, synthesis, physicochemical and pharmacological profiling of 7-hydroxy-5-oxopyrazolo[4,3-b]pyridine-6-carboxamide derivatives with anti-osteoarthritic activity in vivo, *J. Med. Chem.* 63 (13) (2020) 7369–7391, <https://doi.org/10.1021/acs.jmedchem.0c00595>.
- [20] A. Parlar, S.O. Arslan, M.F. Doğan, S.A. Çam, A. Yalçın, E. Elibol, M.K. Özer, F. Üçkardeş, H. Kara, The exogenous administration of CB2 specific agonist, GW405833, inhibits inflammation by reducing cytokine production and oxidative stress, *Exp. Ther. Med.* 16 (2018) 4900–4908, <https://doi.org/10.3892/etm.2018.6753>.
- [21] A. Sophocleous, A.E. Börjesson, D.M. Salter, S.H. Ralston, The type 2 cannabinoid receptor regulates susceptibility to osteoarthritis in mice, *Osteoarthr. Cartil.* 23 (9) (2015) 1586–1594, <https://doi.org/10.1016/j.joca.2015.04.020>.
- [22] S.L. Dunn, J.M. Wilkinson, A. Crawford, C.L. Le Maitre, R.A.D. Bunning, Cannabinoid WIN-55,212-2 mesylate inhibits interleukin-1 $\beta$  induced matrix metalloproteinase and tissue inhibitor of matrix metalloproteinase expression in human chondrocytes, *Osteoarthr. Cartil.* 22 (2014) 133–144, <https://doi.org/10.1016/j.joca.2013.10.016>.
- [23] L.M. Luttrell, R.J. Lefkowitz, The role of  $\beta$ -arrestins in the termination and transduction of G-protein-coupled receptor signals, *J. Cell. Sci.* 115 (3) (2002) 455–465.
- [24] J. De Sousa Valente, The pharmacology of pain associated with the monoiodoacetate model of osteoarthritis, *Front. Pharmacol.* 10 (2019), <https://doi.org/10.3389/fphar.2019.00974>.
- [25] C. Guingamp, P. Gegout-Pottie, L. Philippe, B. Terlain, P. Netter, P. Gillet, Monoiodoacetate-induced experimental osteoarthritis: a dose-response study of loss of mobility, morphology, and biochemistry, *Arthritis Rheum.* 40 (1997) 1670–1679, [https://doi.org/10.1002/1529-0131\(199709\)40:9&1670::AID-ART17&3.0.CO;2-W](https://doi.org/10.1002/1529-0131(199709)40:9&1670::AID-ART17&3.0.CO;2-W).
- [26] M. Bryk, J. Chwastek, M. Kostrzewa, J. Mlost, A. Pędracka, K. Starowicz, Alterations in anandamide synthesis and degradation during osteoarthritis progression in an animal model, *Int. J. Mol. Sci.* 21 (2020) 7381, <https://doi.org/10.3390/ijms21197381>.
- [27] N. Malek, M. Mrugała, W. Makuch, N. Kolosowska, B. Przewlocka, M. Binkowski, M. Czaja, E. Morera, V. Di Marzo, K. Starowicz, A multi-target approach for pain treatment: dual inhibition of fatty acid amide hydrolase and TRPV1 in a rat model of osteoarthritis, *Pain* 156 (2015) 890–903, <https://doi.org/10.1097/j.pain.000000000000132>.
- [28] N.J. Barton, I.T. Strickland, S.M. Bond, H.M. Brash, S.T. Bate, A.W. Wilson, I. P. Chessell, A.J. Reeve, D.S. McQueen, Pressure application measurement (PAM): a novel behavioural technique for measuring hypersensitivity in a rat model of joint pain, *J. Neurosci. Methods* 163 (2007) 67–75, <https://doi.org/10.1016/j.jneumeth.2007.02.012>.
- [29] Ł. Cyganik, M. Binkowski, G. Kokot, T. Rusin, P. Popik, F. Bolechala, R. Nowak, Z. Wrobel, A. John, Prediction of Young's modulus of trabeculae in microscale using macro-scale's relationships between bone density and mechanical properties, *J. Mech. Behav. Biomed. Mater.* 36 (2014) 120–134, <https://doi.org/10.1016/j.jmbbm.2014.04.011>.
- [30] X.X. Peng, R.L. Zhao, W. Song, H.R. Chu, M. Li, S.Y. Song, G.Z. Li, D.C. Liang, Selection of suitable reference genes for normalization of quantitative real-time PCR in cartilage tissue injury and repair in rabbits, *Int. J. Mol. Sci.* 13 (2012) 14344–14355, <https://doi.org/10.3390/ijms131114344>.
- [31] M. Pombo-Suarez, M. Calaza, J.J. Gomez-Reino, A. Gonzalez, Reference genes for normalization of gene expression studies in human osteoarthritic articular cartilage, *BMC Mol. Biol.* 9 (2008) 17, <https://doi.org/10.1186/1471-2199-9-17>.
- [32] J. Mlost, M. Kostrzewa, N. Malek, K. Starowicz, J. Mlost, M. Kostrzewa, N. Malek, K. Starowicz, Molecular understanding of the activation of CB1 and blockade of TRPV1 receptors: implications for novel treatment strategies in osteoarthritis, *Int. J. Mol. Sci.* 19 (2018) 342, <https://doi.org/10.3390/ijms19020342>.
- [33] J. Mlost, A. Waşik, J.T. Michaluk, L. Antkiewicz-Michaluk, K. Starowicz, Changes in monoaminergic neurotransmission in an animal model of osteoarthritis: the role of endocannabinoid signaling, *Front. Mol. Neurosci.* 11 (2018) 466, <https://doi.org/10.3389/fnmol.2018.00466>.
- [34] K.M. Raehal, L.M. Bohn,  $\beta$ -arrestins: Regulatory role and therapeutic potential in opioid and cannabinoid receptor-mediated analgesia, *Handb. Exp. Pharmacol.* 219 (2014) 427–443, [https://doi.org/10.1007/978-3-642-41199-1\\_22](https://doi.org/10.1007/978-3-642-41199-1_22).
- [35] A. Pajak, M. Kostrzewa, N. Malek, M. Korostynski, K. Starowicz, Expression of matrix metalloproteinases and components of the endocannabinoid system in the knee joint are associated with biphasic pain progression in a rat model of osteoarthritis, *J. Pain Res.* 10 (2017) 1973–1989, <https://doi.org/10.2147/JPR.S132682>.
- [36] C. La Porta, S.A. Bura, J. Llorente-Onaindia, A. Pastor, F. Navarrete, M.S. García-Gutiérrez, R. De la Torre, J. Manzanares, J. Monfort, R. Maldonado, Role of the endocannabinoid system in the emotional manifestations of osteoarthritis pain, *Pain* 156 (2015) 2001–2012, <https://doi.org/10.1097/j.pain.0000000000000260>.
- [37] C. La Porta, S.A. Bura, A. Aracil-Fernandez, J. Manzanares, R. Maldonado, Role of CB1 and CB2 cannabinoid receptors in the development of joint pain induced by monosodium iodoacetate, *Pain* 154 (2013) 160–174, <https://doi.org/10.1016/j.pain.2012.10.009>.
- [38] O. Ofek, M. Karsak, N. Leclerc, M. Fogel, B. Frenkel, K. Wright, J. Tam, M. Attar-Namdar, V. Kram, E. Shohami, R. Mechoulam, A. Zimmer, I. Bab, Peripheral cannabinoid receptor, CB2, regulates bone mass, *Proc. Natl. Acad. Sci. U. S. A.* 103 (3) (2006) 696–701, <https://doi.org/10.1073/pnas.0504187103>.
- [39] A. Sophocleous, E. Landao-Bassonga, R.J. Van't Hof, A.I. Idris, S.H. Ralston, The type 2 cannabinoid receptor regulates bone mass and ovariectomy-induced bone loss by affecting osteoblast differentiation and bone formation, *Endocrinology* 152 (2011) 2141–2149, <https://doi.org/10.1210/en.2010-0930>.
- [40] X.Q. Qu, W.J. Wang, S.S. Tang, Y. Liu, J.L. Wang, Correlation between interleukin-6 expression in articular cartilage bone and osteoarthritis, *Genet. Mol. Res.* 14 (4) (2015) 14189–14195, <https://doi.org/10.4238/2015.November.13.2>.
- [41] M. Sabatini, C. Lesur, M. Thomas, A. Chomel, P. Anract, G. De Nanteuil, P. Pastoureau, Effect of inhibition of matrix metalloproteinases on cartilage loss in vitro and in a guinea pig model of osteoarthritis, *Arthritis Rheum.* 52 (1) (2005) 171–180, <https://doi.org/10.1002/art.20900>.
- [42] D. Piecha, J. Weik, H. Kheil, G. Becher, A. Timmermann, A. Jaworski, M. Burger, M.W. Hofmann, Novel selective MMP-13 inhibitors reduce collagen degradation in bovine articular and human osteoarthritis cartilage explants, *Inflamm. Res.* 59 (5) (2010) 379–389, <https://doi.org/10.1007/s00011-009-0112-9>.
- [43] L.M. Coussens, B. Fingleton, L.M. Matrisian, Matrix metalloproteinase inhibitors and cancer: trials and tribulations, *Science* (80-.) 295 (5564) (2002) 2387–2392, <https://doi.org/10.1126/science.1067100>.
- [44] R. Renkiewicz, L. Qiu, C. Lesch, X. Sun, R. Devalaraja, T. Cody, E. Kaldjian, H. Welgus, V. Baragi, Broad-spectrum matrix metalloproteinase inhibitor marimastat-induced musculoskeletal side effects in rats, *Arthritis Rheum.* 48 (6) (2003) 1742–1749, <https://doi.org/10.1002/art.11030>.
- [45] A. Latourte, C. Cherifi, J. Maillet, H.K. Ea, W. Bouaziz, T. Funck-Brentano, M. Cohen-Solal, E. Hay, P. Richette, Systemic inhibition of IL-6/Stat3 signalling protects against experimental osteoarthritis, *Ann. Rheum. Dis.* 76 (4) (2017) 748–755, <https://doi.org/10.1136/annrheumdis-2016-209757>.
- [46] C.T.G. Appleton, S.E. Usmani, M.A. Pest, V. Pitelka, J.S. Mort, F. Beier, Reduction in disease progression by inhibition of transforming growth factor  $\alpha$ -CCL2 signaling in experimental posttraumatic osteoarthritis, *Arthritis Rheumatol.* (Hoboken, N.J.) 67 (10) (2015) 2691–2701, <https://doi.org/10.1002/art.39255>.
- [47] K.M.C. Lee, V. Prasad, A. Achuthan, A.J. Fleetwood, J.A. Hamilton, A.D. Cook, Targeting GM-CSF for collagenase-induced osteoarthritis pain and disease in mice, *Osteoarthr. Cartil.* 28 (4) (2020) 486–491, <https://doi.org/10.1016/j.joca.2020.01.012>.
- [48] M.C. Lee, R. Saleh, A. Achuthan, A.J. Fleetwood, I. Förster, J.A. Hamilton, A. D. Cook, CCL17 blockade as a therapy for osteoarthritis pain and disease, *Arthritis Res. Ther.* 20 (1) (2018), 62, <https://doi.org/10.1186/s13075-018-1560-9>.
- [49] X.H. Liu, A. Kirschenbaum, S. Yao, A.C. Levine, Cross-talk between the interleukin-6 and prostaglandin E2 signaling systems results in enhancement of osteoclastogenesis through effects on the osteoprotegerin/receptor activator of nuclear factor- $\kappa$ B (RANK) ligand/RANK system, *Endocrinology* 146 (4) (2005) 1991–1998, <https://doi.org/10.1210/en.2004-1167>.
- [50] S. Goodman, T. Ma, M. Trindade, T. Ikenoue, I. Matsuura, N. Wong, N. Fox, M. Genovese, D. Regula, R.L. Smith, COX-2 selective NSAID decreases bone ingrowth in vivo, *J. Orthop. Res.* 20 (6) (2002) 1164–1169, [https://doi.org/10.1016/S0736-0266\(02\)00079-7](https://doi.org/10.1016/S0736-0266(02)00079-7).
- [51] M. Kellinsalmi, V. Parikka, J. Risteli, T. Hentunen, H.V. Leskelä, S. Lehtonen, K. Selander, K. Väänänen, P. Lehenkari, Inhibition of cyclooxygenase-2 down-regulates osteoclast and osteoblast differentiation and favours adipocyte formation in vitro, *Eur. J. Pharmacol.* 572 (2–3) (2007) 102–110, <https://doi.org/10.1016/j.ejphar.2007.06.030>.
- [52] C.O. Bingham, S.S. Smugar, H. Wang, A.M. Tershakovec, Early response to COX-2 inhibitors as a predictor of overall response in osteoarthritis: pooled results from two identical trials comparing etoricoxib, celecoxib and placebo, *Rheumatology* 48 (9) (2009) 1122–1127, <https://doi.org/10.1093/rheumatology/kep184>.
- [53] T. Dimitroulas, R.V. Duarte, A. Behura, G.D. Kitas, J.H. Raphael, Neuropathic pain in osteoarthritis: a review of pathophysiological mechanisms and implications for treatment, *Semin. Arthritis Rheum.* 44 (2) (2014) 145–154, <https://doi.org/10.1016/j.semarthrit.2014.05.011>.
- [54] R. Gruber, F. Karreth, M.B. Fischer, G. Watzek, Platelet-released supernatants stimulate formation of osteoclast-like cells through a prostaglandin/RANKL-dependent mechanism, *Bone* 30 (2002) 726–732, [https://doi.org/10.1016/S8756-3282\(02\)00697-X](https://doi.org/10.1016/S8756-3282(02)00697-X).
- [55] C. Karlsson, T. Dehne, A. Lindahl, M. Brittberg, A. Pruss, M. Sittinger, J. Ringe, Genome-wide expression profiling reveals new candidate genes associated with osteoarthritis, *Osteoarthr. Cartil.* 18 (4) (2010) 581–592, <https://doi.org/10.1016/j.joca.2009.12.002>.
- [56] W. Udomsinprasert, A. Jinawath, N. Teerawattanaopong, S. Honsawek, Interleukin-34 overexpression mediated through tumor necrosis factor- $\alpha$  reflects severity of synovitis in knee osteoarthritis, *Sci. Rep.* 10 (1) (2020), 7987, <https://doi.org/10.1038/s41598-020-64932-2>.
- [57] S.L. Wang, R. Zhang, K.Z. Hu, M.Q. Li, Z.C. Li, Interleukin-34 synovial fluid was associated with knee osteoarthritis severity: a cross-sectional study in knee osteoarthritis patients in different radiographic stages, *Dis. Markers* 2018 (2018), 2095480, <https://doi.org/10.1155/2018/2095480>.
- [58] A.G. Clark, J.M. Jordan, V. Vilim, J.B. Renner, A.D. Dragomir, G. Luta, V.B. Kraus, Serum cartilage oligomeric matrix protein reflects osteoarthritis presence and severity: the Johnston County Osteoarthritis Project, *Arthritis Rheum.* 42 (11) (1999) 2356–2364, [https://doi.org/10.1002/1529-0131\(199911\)42:11<2356::AID-ANR14>3.0.CO;2-R](https://doi.org/10.1002/1529-0131(199911)42:11<2356::AID-ANR14>3.0.CO;2-R).
- [59] J.M. Hoch, C.G. Mattacola, J.M. Medina McKeon, J.S. Howard, C. Lattermann, Serum cartilage oligomeric matrix protein (sCOMP) is elevated in patients with

- knee osteoarthritis: a systematic review and meta-analysis, *Osteoarthr. Cartil.* 19 (12) (2011) 1396–1404, <https://doi.org/10.1016/j.joca.2011.09.005>.
- [60] E.J. Murphy, G. Barcelo-Coblijn, B. Binas, J.F.C. Glatz, Heart fatty acid uptake is decreased in heart fatty acid-binding protein gene-ablated mice, *J. Biol. Chem.* 279 (33) (2004) 34481–34488, <https://doi.org/10.1074/jbc.M314263200>.
- [61] E. Toyoda, M. Sato, T. Takahashi, M. Maehara, E. Okada, S. Wasai, M. Watanabe, H. Iijima, K. Nonaka, Y. Kawaguchi, Transcriptomic and proteomic analyses reveal the potential mode of action of chondrocyte sheets in hyaline cartilage regeneration, *Int. J. Mol. Sci.* 21 (1) (2020), 149, <https://doi.org/10.3390/ijms21010149>.
- [62] M. Soethoudt, U. Grether, J. Fingerle, T.W. Grim, F. Fezza, L. De Petrocellis, C. Ullmer, B. Rothenhäusler, C. Perret, N. Van Gils, D. Finlay, C. Macdonald, A. Chicca, M.D. Gens, J. Stuart, H. De Vries, N. Mastrangelo, L. Xia, G. Alachouzos, M.P. Baggelaar, A. Martella, E.D. Mock, H. Deng, L.H. Heitman, M. Connor, V. Di Marzo, J. Gertsch, A.H. Lichtman, M. Maccarrone, P. Pacher, M. Glass, M. Van Der Stelt, Cannabinoid CB2 receptor ligand profiling reveals biased signalling and off-target activity, *Nat. Commun.* 8 (2017) 1–14, <https://doi.org/10.1038/ncomms13958>.
- [63] J. Ferreira-Gomes, S. Adães, R.M. Sousa, M. Mendonça, J.M. Castro-Lopes, Dose-dependent expression of neuronal injury markers during experimental osteoarthritis induced by monoiodoacetate in the rat, *Mol. Pain* 8 (2012) 50, <https://doi.org/10.1186/1744-8069-8-50>.
- [64] J.J. Burston, D.R. Sagar, P. Shao, M. Bai, E. King, L. Brailsford, J.M. Turner, G. J. Hathway, A.J. Bennett, D.A. Walsh, D.A. Kendall, A. Lichtman, V. Chapman, Cannabinoid CB2 receptors regulate central sensitization and pain responses associated with osteoarthritis of the knee joint, *PLoS One* 8 (2013), e80440, <https://doi.org/10.1371/journal.pone.0080440>.